

# Cardiac Phase Extraction in IVUS Sequences using 1-D Gabor Filters

Joel Barajas, Karla L Caballero, Oriol Rodriguez and Petia Radeva

**Abstract**—A main issue in the automatic analysis of Intravascular Ultrasound (IVUS) images is the presence of periodic changes provoked by heart motion during the cardiac cycle. Although the Electrocardiogram (ECG) signal can be used to gate the sequence, few IVUS systems incorporate the ECG-gating option, and the synchronization between them implies several issues. In this paper, we present a fast and robust method to assign a phase in the cardiac cycle to each image in the sequence directly from in vivo clinical IVUS sequences. It is based on the assumption that the vessel wall is significantly brighter than the blood in each IVUS beam. To guarantee stability in this assumption, we use normalized reconstructed images. Then, the wall boundary is extracted for all the radial beams in the sequence and a matrix with these positions is formed. This matrix is filtered using a bank of 1-D Gabor filters centered at the predominant frequency of a given number of windows in the sequence. After filtering, we combine the responses to obtain a unique phase within the cardiac cycle for each image. For this study, we gate the sequence to make the sequence comparable with other ones of the same patient. The method is tested with 12 pullbacks of real patients and 15 synthetic tests.

## I. INTRODUCTION

Intravascular Ultrasound (IVUS) represents a powerful tool to explore the coronary vessels in deep detail. It provides high-resolution tomographic images of the vessel which allow the quantification of lumen volume, plaque components, and vessel shape, among others [Mario et al., 2005]. These measurements are of great interest in the diagnosis of certain pathologies such as atherosclerosis, stenosis, and coronary artery disease [Nissen et al., 1991].

The IVUS study consists in the introduction of a catheter inside the coronary vessels to perform an exploration. Here, an ultrasound emitter and a transducer are attached to the catheter. The emitter shoots a number of beams radially whose reflections are collected by the transducer giving a description of the morphology and tissue nature based on their intensity [Caballero et al., 2006]. An IVUS exploration is performed by a uniform-speed motorized pullback of the catheter generating a sequence of images.

This work was supported in part by a research grant from projects TIN2006-15308-C02, FIS-PI061290, by the Generalitat of Catalunya under the FI grant and by the Spanish Ministry of Education and Sciences (MEC) under the FPU grant Ref: AP2005-0926

Joel Barajas and Kala L Caballero are with the Computer Vision Center, Autonomous University of Barcelona, Edificio O Campus UAB, 08193 Bellaterra, Spain joelbz@cvc.uab.es, klcaballero@cvc.uab.es

Petia Radeva are with the Department Mathematical Analysis, University of Barcelona, Barcelona, Spain and the Computer Vision Center. petia@cvc.uab.es

Oriol Rodriguez is with the Hemodynamics Department, Hospital Universitari German Trias i Pujol, Badalona, Spain

However, there are periodic changes in the position of the catheter in the vessel due to the cardiac motion. It provokes a serious destabilization in the analysis of the IVUS sequence since there is not a continuous exploration. Several techniques have been proposed to overcome this issue. Electrocardiogram (ECG) gated method has been suggested where the ECG signal is used to trigger the acquisition once per cardiac period [Bruning et al., 1998]. Nevertheless, the recording of the ECG is rarely implemented in IVUS commercial equipments and it suggests a good synchronization between the acquisitions. In addition, it limits the study to only one image per cardiac cycle and there are studies which have explored more than one frame in the cycle [Veress et al., 2002]. On the other hand, some approaches have been designed to subtract the cardiac motion based on the IVUS sequence itself [Zhu et al., 2003], [Winter et al., 2004]. Nonetheless, the methods proposed assume small variations in the cardiac frequency and only take into account the frequency peak obtained from the gray values of the longitudinal view [Winter et al., 2004]. It generates errors when the oscillations are not well defined in this view. Other methods assume that the IVUS sequence experiments small structure changes and the motion is corrected by registration based on a spectral analysis of each image [Hernandez et al., 2006]. However, a high echogenic plaque in the oscillation might affect drastically the vessel morphology undermining the efficiency of these methods.

In this paper, we propose a novel method to extract the cardiac motion and subtract its effects in the IVUS pullbacks. A fast wall detection is applied for all the beam reflections in the complete sequence offering the advantage of analyzing all the available longitudinal views from the polar representation. Thus, any change in the structure, plaque, or morphology, that affects the vessel wall related with the cardiac frequency is used. Moreover, if sharp changes are present they will reflect more energy to the frequency peak and cardiac phase detection. To perform a local analysis of the cardiac frequency, a set of 1-D Gabor filters is employed. The system has demonstrated to be robust in 12 pullbacks of real patients and in 15 synthetic tests varying the cardiac frequency and adding noise to the periodic pattern. In section 2, the wall detection and filtering issues are detailed. In section 3, relevant results are shown for real and synthetic data. Finally, in section 4 a conclusion and future work are mentioned.

## II. METHODS

One of the main problems in the analysis of IVUS images is the high variability among different patients. However,

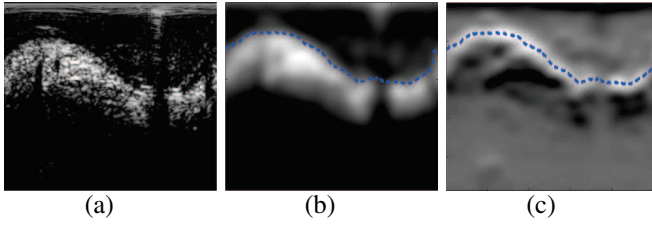


Fig. 1. Example of wall detection for a polar image. The dashed line represents the wall boundary detected. (a) Original polar IVUS image. (b) Smoothed image used to detect the wall. (c) Derivative used along the columns to find the inflection points  $w$ .

there has been proved that a significant contribution of this variability comes from the nonlinear radial-based contrast performed by the IVUS system [Caballero et al., 2006]. This feature allows physicians to customize the visualization of a sequence by radial regions which introduces an important level of variability. Therefore, we have determined to use IVUS images reconstructed from the raw Radio Frequency (RF) reflections collected by the catheter transducer since they have demonstrated to be more robust for automatic analysis [Caballero et al., 2006].

#### A. Wall Boundary Estimation

In general, the mean value of the pixels in the wall is considerably brighter than in the blood in spite of the texture [Zhu et al., 2003]. Because we are using reconstructed images, a good level of consistency in this assumption is assured by normalizing the reconstruction parameters [Caballero et al., 2006]. Thus, the polar IVUS images can be smoothed to diminish the texture highlighting the difference between the blood and the vessel wall. To achieve this task, we employ a Gaussian filter. Fig. 1(a) shows an example of the smoothing used.

To estimate the wall boundary, we extract the inflection point  $w$  related with the highest value of the radial reflections. If there are small maxima near this value, the point where the derivative is the highest is chosen as  $w$ . When the derivative at  $w$  is under a certain threshold, the wall is considered as not well defined and the value calculated in the previous reflection is assigned. It helps to deal with bifurcations as well as the guide artifact in rotational catheters. If more than one maximum are found and their values associated with are similar, the nearest to the one found in the previous reflection is designated. Fig. 1 displays one example of the inflection points estimated for a polar image.

When high or mid echogenic plaque is present, the wall detection is moved to its boundary. Although it is not strictly the wall boundary, it is subjected to a similar motion pattern as the rest of the vessel. Moreover, the presence of plaque implicitly represents a reliable landmark to find the cardiac frequency and estimate the position of the image inside the cardiac cycle.

This wall detection is applied for all the radial reflections in the IVUS sequence. Then, an image  $I_w$  is generated by arranging the distance between the image center and the boundary estimation  $w$ . Let  $\theta$  be the angle in the polar image,

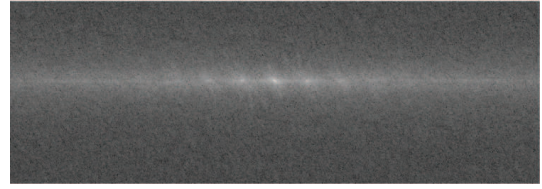


Fig. 2. Typical Spectrum in Decibels of  $I_w$

and  $n$  the frame in the time along the sequence. Then, the image  $I_w$  is defined as:

$$I_w = \begin{bmatrix} w_{1,1} & w_{1,2} & \dots & w_{1,L_n-1} & w_{1,L_n} \\ w_{2,1} & w_{2,2} & \dots & w_{2,L_n-1} & w_{2,L_n} \\ \vdots & \vdots & \ddots & \vdots & \vdots \\ w_{N_\theta-1,1} & w_{N_\theta-1,2} & \dots & w_{N_\theta-1,L_n-1} & w_{N_\theta-1,L_n} \\ w_{N_\theta,1} & w_{N_\theta,2} & \dots & w_{N_\theta,L_n-1} & w_{N_\theta,L_n} \end{bmatrix}$$

where  $N_\theta$  is the number of angles  $\theta$  the vessel is divided into in the polar image, and  $L_n$  is the length of the sequence in frames  $n$ .

#### B. Cardiac Frequency Filtering

Once  $I_w$  has been calculated, we have the wall boundary oscillations in each longitudinal view along its rows. Although their phases depend on the  $\theta$  taken, we can look for the one where the cardiac frequency is highest for each frame  $n$ . Finally, a unique phase in the cardiac cycle for each image can be assigned.

Due to the cardiac oscillations, the spectrum of  $I_w$  shows a peak at a global cardiac frequency. Fig. 2 shows a typical spectrum of  $I_w$ . Nevertheless, assuming a unique frequency is fallacious since variations in this value are probable. To solve this issue, we extract the cardiac frequency  $F_c$  from the spectrum, then a number of periods  $T$  is established to divide the sequence and find the predominant frequency  $F_i$  in these windows yielding a number of frequencies  $N_F$ . We have employed a 1-D Gabor filter for each  $F_i$  which are convoluted with the rows of  $I_w$  independently along the time.

The Gabor filters have been shown to have optimal combined localization in both the spatial and the spatial-frequency domain [Kamarainen et al., 2006], [Daugman, 1985]. In certain applications this filtering technique has demonstrated to be robust and fast [Tsai and Lee, 2002]. In 1-D, it is defined as:

$$h(n) = \frac{1}{\sqrt{2\pi}\sigma} e^{-\frac{1}{2}\left(\frac{n}{\sigma}\right)^2} e^{-j2\pi F_i n},$$

where  $\sigma$  represents the bandwidth and  $F_i$  the frequency centered. For our case  $\sigma = F_i^{-1}$ .

Let  $I_w^{F_i}$  be  $I_w$  filtered along the rows by a Gabor filter  $h_{F_i}$  whose central frequency is  $F_i$ . We use the magnitude response  $|I_w^{F_i}|$  to measure the frequency content at a given frame  $n$  for each angle  $\theta$ . The phase response  $\angle I_w^{F_i}$  is the relative position of frame  $n$  in the cardiac cycle. Fig. 3 illustrates the real part of a filtered response and its correlation with the original signal.

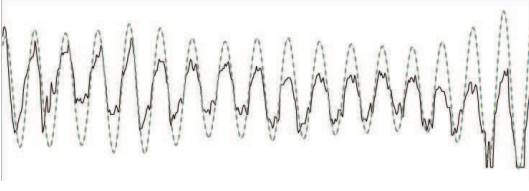


Fig. 3. Real response of a segment of a row of  $I_{F_i}$  after filtering. The solid wave represents the values in  $I_w$ . The dashed wave is the real filter response.

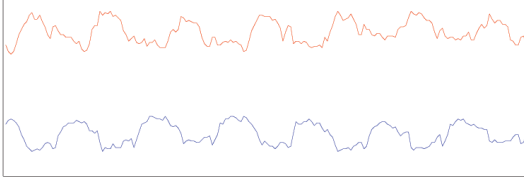


Fig. 4. Unsynchronized rows of  $I_w$  of different longitudinal views.

Given a number of frequencies  $N_F$ , we have  $N_F$  filtered images  $I_w^{F_i}$ . Hence, the final response is defined by:

$$I_F = \max\{I_w^{F_1}, I_w^{F_2}, \dots, I_w^{F_{N_F}}\}$$

where the max operator is computed using the magnitude,  $|I_w^{F_i}|$ , of the complex filtered responses.

### C. Phase Estimation and Gating

From  $I_F$  we have a set of  $N_\theta$  complex values  $\theta$  along the columns for each image  $n$  in the sequence. We know that each frame has a unique phase value in the cardiac cycle. Thus, to assign a single response by frame, the highest magnitude by columns is obtained assuming that at this angle  $\theta$  it experiments the highest effect due to the cardiac frequency. Let  $\mathbf{x}_F$  denote the 1-D filtered response for an IVUS sequence of  $L_n$  frames, then it is expressed as:

$$\mathbf{x}_F = \left[ \max\{\mathbf{c}_F^1\}, \max\{\mathbf{c}_F^2\}, \dots, \max\{\mathbf{c}_F^{L_n}\} \right]^T$$

$$\mathbf{c}_F^n = I_F([1, N_\theta], n).$$

Since the values in  $\mathbf{x}_F$  come from different rows  $\theta$ , we can expect that the phase values  $\angle \mathbf{x}_F(n)$  and  $\angle \mathbf{x}_F(n+1)$  are unsynchronized. This effect is related with the geometry of the vessel wall detected. In Fig. 4 a section of two opposite rows,  $\theta$  and  $\theta + N_\theta/2$ , of  $I_w$  are shown. Here, the difference in phase is near to  $\pi$  radians.

To synchronize  $\mathbf{x}_F$ , we correct the phase shift between frame  $n$  and  $n+1$  such that the sequence is synchronized with the first frame. To do so, a cardiac period  $T_c$  centered in  $n$  is extracted from the rows  $i_n$  and  $i_{n+1}$  of  $I_F$  which correspond to the indices of highest magnitude in  $\mathbf{c}_F^n$  and  $\mathbf{c}_F^{n+1}$  respectively. We place the phases in the complex unitary circle, obtained the complex mean, and extracted its phase. Hence, the synchronized filtered response  $\mathbf{x}'_F$  is:

$$\phi = \angle \sum_{j=n-T_c/2}^{n+T_c/2} \frac{I_F(i_n, j)}{I_F(i_{n+1}, j)},$$

$$\mathbf{x}'_F(n+1) = e^{j\phi} \mathbf{x}_F(n+1),$$

for  $n = \frac{T_c}{2}, \frac{T_c}{2} + 1, \dots, L_n - \frac{T_c}{2}$ . When  $L_n - \frac{T_c}{2} < n < \frac{T_c}{2}$ ,  $\phi$  is estimated using the last or first  $T$  elements in  $I_F$ . In order to synchronize  $\mathbf{x}'_F$  with a fixed vessel angle, the first frame  $\mathbf{x}_F(1)$  is referred to the row  $\theta = 1$  which corresponds to the twelve o'clock angle in the cartesian images.

Once a phase value has been assigned to each IVUS image, we need to look for the desired phase in the cardiac cycle to gate. Therefore, the end-diastole can be localized by looking for its associated phase to build a sequence free of the cardiac frequency motion.

## III. RESULTS

We tested our method with real and synthetic sequences. The synthetic sequences are used to validate while the results in real patients are shown. A Galaxy IVUS equipment from Boston Scientific was used. The RF channel available in the equipment was employed to acquire the signal and create the images as explained in [Caballero et al., 2006]. For this system  $N_\theta = 256$ , which is the number of RF beams by image with a frame rate  $30 \text{ frames/s}$ . The depth used is  $4.48 \text{ mm}$  with a resolution of  $0.0174 \text{ mm/pixel}$ . The number of periods to divide the sequence and find the predominant frequency was fixed to  $T = 5$ .

### A. Validation Protocol

To validate this approach, a real IVUS polar image is taken and rotated periodically at a certain frequency  $F_s$  with a triangle pattern having a peak value  $P_s$ . Through the factor  $N_s$ , a random uniformly distributed noise is introduced in the range  $[-N_s P_s, N_s P_s]$  to the rotation pattern where  $0 \leq N_s \leq 1$ . In addition, we introduced a frequency pattern along the time to evaluate the robustness of the method in changes of cardiac frequency. The root mean square error between the introduced pattern and the one reported by the method in  $\text{Hz}$ ,  $E_{rms}^F$  after gating is used as accuracy measure.  $E_{rms}^T$  is the error in  $\text{frames/s}$ .

### B. Synthetic Tests

We created 15 synthetic patterns to test the efficiency of the gating by comparing the period between the frames picked and the pattern introduced. Results for some of the most representative tests are depicted in Fig. 5. We used a peak value  $P_s = \pi/2$ . Although the noise factors  $N_s$  are high  $[0.3, 0.5]$ , the errors reported  $E_{rms}^T = [1, 2] \text{ frames/s}$  are acceptable given the frame rate assumed. A single decrease in frequency Fig. 5(a) and a random variation from a range Fig. 5(b)(c) are some of the patterns tested. Although we can expect a lower and more constant variation in cardiac frequency, the tests were performed to evaluate the systems in extreme cases.

### C. Pullback Sequences of Real Patients

The method was tested with 12 pullbacks of real patients. Some longitudinal views of gated sequences are shown in Fig. 6. There are regions where the presence of plaque oscillates while the pullback is performed. Although the morphology changes considerably, the cardiac phase detection is achieved. To compute the wall detection, we

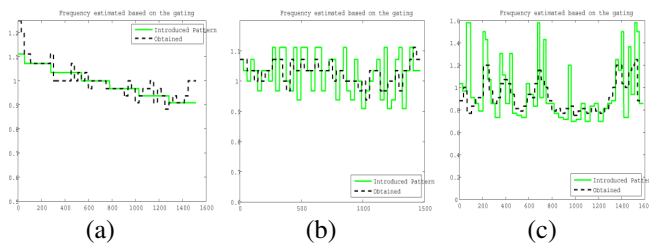


Fig. 5. Representative frequency patterns tested. The solid line represents the frequency introduced and the dashed one the frequency obtained.  $y$ -axis frequency in  $Hz$ .  $x$ -axis frame sequence number. (a) Gradual decrease in  $f = [1.1, 0.9]Hz$  with a noise factor  $N_S = 0.4$ .  $E_{rms}^F = 0.0399Hz$  and  $E_{rms}^T = 1.1966frames/s$ . (b) Randomly distributed frequency pattern  $f = [0.7, 1.3]Hz$ ,  $N_S = 0.3$ .  $E_{rms}^F = 0.0657Hz$  and  $E_{rms}^T = 1.9705frames/s$ . (c) Randomly distributed frequency pattern  $f = [0.7, 1.6]Hz$ ,  $N_S = 0.45$ .  $E_{rms}^F = 0.0535Hz$  and  $E_{rms}^T = 1.6043frames/s$ .

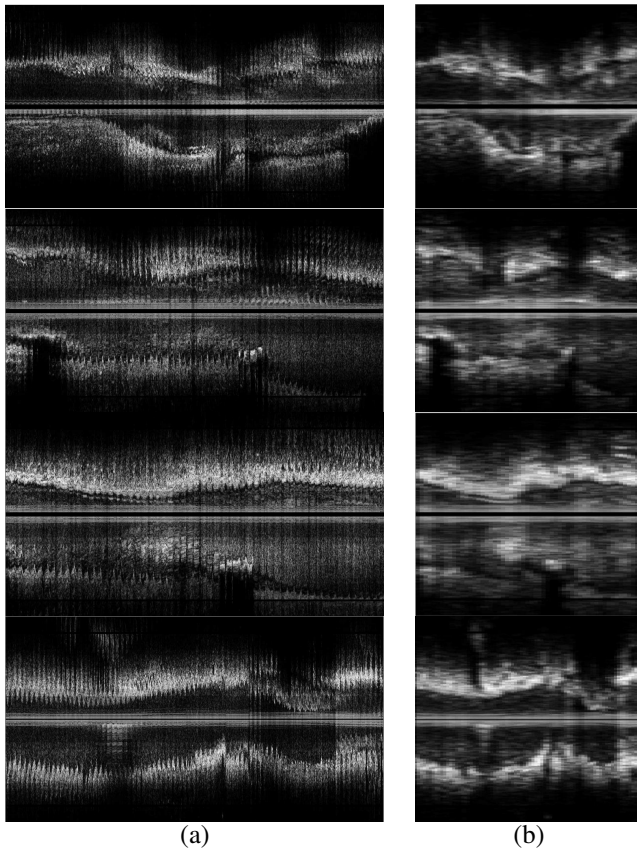


Fig. 6. Longitudinal views of 4 real IVUS pullbacks. (a) Original sequence. (b) After gating.

assume the vessel mean brighter than the blood. Even when this difference is lower in certain fragments, the method successfully gated the sequence. It is because only one wall point in the polar image is needed to detect the frequency. Hence, if the oscillations are present in at least one angle direction of the sequence the method will obtain the cardiac phase successfully.

#### IV. CONCLUSION AND FUTURE WORK

A novel method to extract the cardiac phase for each image in the IVUS sequence has been presented. It has demonstrated to be robust in cardiac frequency changes with

considerable level of noise in the pattern. The method has been shown to be effective when there are sharp changes in the vessel morphology due to the cardiac motion. The method implicitly takes advantage when high echogenic plaques appear and disappear due to the cardiac motion.

In this paper, the phase localization is used to gate the IVUS sequence. It reduces the spatial resolution in the vessel position to  $0.5mm$  when the cardiac frequency is  $1Hz$ . For automatic plaque localization and analysis this resolution might be enough. However, in 3-D vessel reconstruction the higher spatial resolution, the more precise the reconstruction has to be. Since we are able to estimate the cardiac phase for each image, a future line is to localize each image not only in the cardiac cycle, but also inside the vessel. The method is strongly based on the presence of oscillations due to the cardiac frequency. If the vessel diameter is small, the periodic motion might decrease, undermining the effectiveness of the method. Nonetheless, the rotational and phase array catheters still introduce these oscillations since they are free inside the vessel during the pullback.

#### REFERENCES

- [Bruning et al., 1998] Bruning, O., Birgelen, C. V., Defeyter, P. J., Lighthart, J., Li, W., Cerruys, P. W., and Roelandt, J. R. T. C. (1998). ECG-gated versus non gated three-dimensional intracoronary ultrasound analysis: Implications for volumetric measurements. *Catheterization and Cardiovascular Diagnosis*, 43:254–260.
- [Bruning et al., 1995] Bruning, O., Birgelen, C. V., Dimario, C., Prati, F., Li, W., Denhoed, W., Patijn, M., Defeyter, P. J., Cerruys, P. W., and Roelandt, J. R. T. C. (1995). Dynamic three-dimensional reconstruction of icus images based on a ecg-gated pullback device. In *Computers in Cardiology*, pages 633–636.
- [Caballero et al., 2006] Caballero, K. L., Barajas, J., Pujol, O., Salvatella, N., and Radeva, P. (2006). In-vivo ivus tissue classification: A comparison between rf signal analysis and reconstructed images. In *CIARP*, pages 137–146.
- [Daugman, 1985] Daugman, J. (1985). Uncertainty relation for resolution in space, spatial frequency, and orientation optimized by two-dimensional visual cortical filters. *Journal of the Optical Society of America*, 2(A):1160–1169.
- [Hernandez et al., 2006] Hernandez, A., Gil, D., Mauri, J., and Radeva, P. (2006). Reducing cardiac motion in ivus sequences. In *Computers in Cardiology*.
- [Kamarainen et al., 2006] Kamarainen, J.-K., Kyrki, V., and Kälviäinen, H. (2006). Invariance properties of Gabor filter based features - overview and applications. *IEEE Trans. on Image Processing*, 15(5):1088–1099.
- [Mario et al., 2005] Mario, C. D., von Birgelen, C., and Prati, F. (2005). Three-dimensional reconstruction of two dimensional intracoronary ultrasound: clinical research tool ? *British Heart Journal*, 73(2):26.
- [Nissen et al., 1991] Nissen, S. E., J.C.Gurley, and Grines, C. (1991). Intravascular ultrasound assesment of lumen size and wall morphology in normal subjects and patients with coronary artery disease. *Circulation*, 84:1087–1099.
- [Tsai and Lee, 2002] Tsai, D. M. and Lee, C. P. (2002). Fast defect detection in textured surfaces using 1d gabor filters. *Int. J. Adv Manuf. Technol.*, 20:664–675.
- [Veress et al., 2002] Veress, A., Weiss, J. A., Gullberg, G. T., Vince, D. G., and Rabbitt, R. D. (2002). Strain measurement in coronary artery using intravascular ultrasound and deformable images. *Journal of Biomechanical Engineering*, 124.
- [Winter et al., 2004] Winter, S. A. D., Hamers, R., and Degertekin, M. (2004). Restrospective image-based gating of intracoronary ultrasound images for improve quantitative analysis: The intelligate method. *Catheterization and Intravascular Intervention*, 61:84–94.
- [Zhu et al., 2003] Zhu, H., Oakeson, K. D., and Freedman, M. H. (2003). Retrieval of cardiac phase from ivus sequences. In *Medical Imaging 2003: Ultrasonic Imaging and Signal Processing*, volume 5035, pages 135–146.